

# Ab initio molecular dynamics simulations of the adsorption of H<sub>2</sub> on palladium surfaces

Axel Groß

*Institut für Theoretische Chemie, Universität Ulm, D-89069 Ulm, Germany*

The interaction of hydrogen represents a model system for the study of the adsorption and absorption at metal surfaces. Theoretical gas-surface dynamics studies have usually concentrated on the adsorption dynamics on clean surfaces. Only recently it has become possible, based on advances in the electronic structure codes and improvements in the computer power, to address the much more complex problem of the adsorption dynamics on precovered surfaces. In this brief review, recent ab initio molecular dynamics studies will be discussed addressing the adsorption dynamics of hydrogen molecules on hydrogen- and sulfur-precovered Pd surfaces. In addition, the relaxation dynamics of the hydrogen atoms after the dissociation on clean Pd(100) will be presented.

PACS numbers: 68.43.Bc, 68.43.Mn, 82.65.+r

## I. INTRODUCTION

The interaction of molecules with surfaces is of importance in many diverse areas such as heterogeneous catalysis, sensing, growth of devices and passivation, just to name a few. The adsorption of hydrogen on metal surfaces has been one of the model system in this field [1–4]. This is due to the fact that this system is well-suited for both experimental as well as theoretical studies. In particular the interaction of hydrogen with palladium surfaces has been studied very intensively [5–27] since this system is of relevance from a fundamental and a technological point of view. This is particularly true in the context of hydrogen storage because hydrogen can absorb huge amounts of hydrogen [28] and can act as a hydrogen sensor [29]. Still, this system is also important with respect to hydrogenation reactions in heterogeneous catalysis.

Hydrogen is rather strongly interacting with palladium. In particular on Pd(110), hydrogen adsorption at higher coverages can induce several different reconstructions as a function of the coverage [14, 23, 26, 27]. Experimentally, however, it is very hard to determine the positions of hydrogen atoms on the reconstructed surfaces because they hardly scatter electrons so that they are almost invisible for experimental methods using electron diffraction techniques. Here, the hydrogen induced polymorphism has been studied in detail by DFT calculations [22, 30] elucidating the geometric and electronic structure of the hydrogen-induced reconstructions.

The fact that hydrogen can take up a large amount of hydrogen has motivated several theoretical studies addressing the energetics of hydrogen absorption in subsurface layers [10, 15, 31–35]. The subsurface sites are found to be energetically less favorable than the adsorption sites on the surface. Therefore, for low coverages hydrogen will always stay on the surface and not penetrate into the bulk. Only if one doses palladium surfaces with more than one monolayer, then hydrogen will start to dissolve into the bulk [21].

The facile incorporation of hydrogen into Pd is the

origin of some confusion about alleged anomalous multilayer relaxation effects. Pd(100) exhibits an unusual outward relaxation of the first layer of Pd(100) [36, 37]. It was speculated that interstitial hydrogen might be one of the possible origins for this anomalous behavior, but the experimental *invisibility* of hydrogen did not allow a verification of this speculation. Only careful experiments avoiding any hydrogen contamination verified that this outward relaxation is the consequence of the presence of subsurface hydrogen [24].

As far as the reactivity of Pd surface with respect to hydrogen is concerned, most studies were concerned with clean Pd surfaces. To the best of my knowledge, so far only one experimental study (Behm *et al.* [38]) determined the sticking probability of hydrogen on Pd(100) as a function of coverage. However, not only the coverage of the considered adsorbens itself can influence the adsorption probability, but also the coadsorption of other species can poison or promote reactions on surfaces. On Pd, in particular the influence of sulfur on the hydrogen-Pd interaction dynamics was studied both experimentally [6, 12, 39, 40] as well as theoretically [40–45], but also CO coadsorption was considered [46].

As far as the first-principles based theoretical description of the H<sub>2</sub>-Pd dynamics on low-index metal surfaces is concerned, it has usually been treated quantum mechanically because of the light mass of hydrogen [1, 7, 47–49], but also classical dynamical studies were performed [11, 17, 18, 20, 50]. In these calculations, all six degrees of freedom of the H<sub>2</sub> molecule were explicitly considered, the substrate degrees of freedom, however, were kept frozen since otherwise the calculations would have been computationally much too expensive. This was justified by the large mass mismatch between hydrogen and metal atoms. In addition, comparisons between six-dimensional quantum and classical calculations showed that the role of quantum effects in the hydrogen adsorption dynamics on surfaces is limited [50, 51].

These simulations are typically performed on parameterized potential energy surfaces [52–56]. If more than six degrees of freedom are involved, the parameterization of

such high-dimensional potential energy surfaces becomes quite cumbersome [57]. Alternatively, *ab initio* molecular dynamics (AIMD) simulations of the adsorption dynamics can be performed. Since in these simulations, the forces necessary to integrate the equations of motion are determined “on the fly” by first-principles calculations, no parameterization of the potential energy surfaces is required. However, in every single time step of the molecular dynamics simulations a converged first-principles electronic structure calculation has to be performed. This results in a considerable computational effort, so that up to recently AIMD simulations were restricted to a small number of trajectories [58, 59].

Fortunately, due to the increase in computer power and the development of more efficient algorithms it has now become possible to determine a statistically meaningful number of AIMD trajectories [60]. This allows to address the adsorption dynamics from first principles in complex systems where many degrees of freedom play a crucial role, such as adsorption on precovered surfaces, but also in systems where the surface recoil cannot be neglected. In this brief review, I will discuss recent AIMD studies of  $H_2$  interacting with precovered Pd surfaces. In addition, I will present studies addressing the hydrogen relaxation dynamics after the dissociative adsorption on Pd.

## II. THEORETICAL METHODS

All the AIMD simulations presented in this review were performed using the periodic DFT code VASP [61] within the generalized gradient approximation (GGA) [62, 63] for the exchange-correlation functional. To reduce the computational effort, the atomic cores were represented either by ultrasoft pseudopotentials [64] or by projected augmented-wave (PAW) potentials [65] allowing a small cutoff energy in the expansion of the one-electron valence states in plane waves. The substrates were modeled by slabs of three to five layers within the supercell approach. The uppermost layers were allowed to move in the simulations in order to enable recoil and energy transfer processes at the surface. The MD simulations were performed using the Verlet algorithm with a time step of 1 fs within the microcanonical ensemble. Typically, all substrate atoms were initially at rest, i.e., the initial surface temperature corresponded to 0 K.

The reaction probabilities were determined by averaging over trajectories with random initial lateral configurations and molecular orientations for one particular kinetic energy. This leads to a statistical error of  $\sigma = \sqrt{s(1-s)}/\sqrt{N}$  where  $s$  is the adsorption probability and  $N$  the number of trajectories. For example, for  $N = 200$  this leads to a statistical error of  $\sigma \leq 0.035$ . It is important to emphasize that the statistical error does not depend on the complexity of the system, i.e., the number of considered dynamical degrees of freedom. It should also be noted that AIMD simulations of reaction probabilities on surfaces are restricted to, say, less than 1000

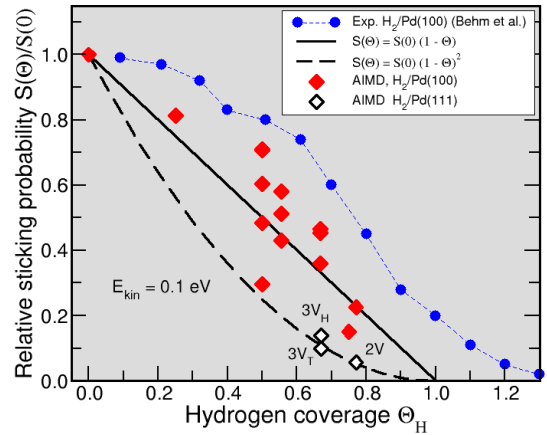


FIG. 1: Relative dissociative adsorption probability of hydrogen on hydrogen-covered Pd(100) determined through AIMD simulations as a function of hydrogen coverage  $\theta_H$  involving different arrangements of the hydrogen. The initial kinetic energy is 0.1 eV.  $2V$ ,  $3V_H$  and  $3V_T$  denote the dimer vacancy and the trimer vacancy centered around a Pd hollow and a Pd top site on Pd(111), respectively. The experimental results [38] were obtained for a temperature of 170 K.

trajectories because of their still considerable computational cost. This results in an absolute statistical error in the reaction probabilities of not less than 0.01 which means that AIMD simulations should only be applied to reactions that have probabilities larger than 0.05.

## III. HYDROGEN DISSOCIATION ON HYDROGEN-PRECOVERED Pd SURFACES

It is rather obvious that the presence of adsorbates on surface modifies the adsorption probability of impinging molecules. First of all, adsorbates lower the number of available sites. Apart from this pure site blocking effect there can be a direct mutual interaction between adsorbates and molecule and an indirect interaction through the modification of the electronic properties of the substrate.

Typically hydrogen atoms on metal surfaces show a mutual repulsion due to dipole-dipole interactions [66] which, together with the site-blocking, should lead to a adsorption probability that decreases with increasing coverage [67]. And indeed, the experiments by Behm *et al.* [38] in which the Pd(100) surface was dosed with hydrogen molecules at a temperature of 170 K find a sticking probability that follows this behavior (see Fig. 1).

Figure 1 also shows the relative sticking probabilities according to AIMD simulations of  $H_2$  impinging with an kinetic energy of 0.1 eV on hydrogen-precovered Pd(100) as a function of the coverage. The results were obtained with  $(2 \times 2)$ ,  $(3 \times 2)$  and  $(3 \times 3)$  surface unit cells for different configurations of the precovered hy-

drogen atoms. In addition, two curves corresponding to  $S(\Theta_H) = S(0)(1 - \Theta_H)$  and  $S(\Theta_H) = S(0)(1 - \Theta_H)^2$  are included which would correspond to the sticking probability if it was determined by pure site-blocking requiring one or two empty sites, respectively.

At low and intermediate coverages, both the calculated as well as the measured sticking probabilities of  $H_2$  at Pd(100) are larger than predicted from a simple site-blocking picture, in particular for  $\Theta_H = 0.5$ . Running additional AIMD trajectories with the substrate kept fixed reveals that it is the energy transfer from the impinging  $H_2$  molecule to the substrate and the rearrangement of the substrate atoms that lead to this enhanced sticking probability compared to pure site blocking [60]. These effects overcompensate the poisoning of the  $H_2$  dissociation caused by the presence of the hydrogen overlayer atoms.

The spread in the calculated sticking probabilities clearly indicates that the sticking probability strongly depends on the particular arrangement of the pre-adsorbed hydrogen atoms [20]. In the experiment, the particular structure of the adsorbed hydrogen could not be specified except for the fact that at low temperatures and intermediate coverages the formation of a  $c(2 \times 2)$  pattern was observed in low-energy electron diffraction (LEED) experiments [38]. Qualitatively, the calculated maximum sticking probabilities per specific coverage trace the measured sticking probabilities, but they are systematically lower. With respect to the discrepancy, it should be noted that the experimental sticking probabilities were obtained for a diffusive gas exposed to the surface at low surface temperatures whereas the calculations were carried out with hyperthermal kinetic energies with surface atoms that were initially at rest, i.e., at a surface temperature of 0 K. In fact, recently MD simulations were performed for  $H_2$  impinging on a frozen hydrogen-precovered Pd(100) surface within a  $(2 \times 2)$  periodicity [20] with a parameterized potential energy surface that was obtained from DFT calculations using a modified corrugation reducing procedure (CRP) [53]. These MD simulations showed that the relative sticking probability depends on the initial kinetic energy. Given these uncertainties in the comparison between theory and experiment, the agreement is considered to be quite satisfactory.

As far as the dependence of the sticking probability on the particular configuration of the preadsorbed hydrogen is concerned, it is usually assumed that two adjacent vacancies, a so-called dimer vacancy, is needed for the dissociative adsorption. This notion which goes back to Langmuir was in fact recently questioned based on STM study addressing the formation of ordered hydrogen layers on Pd(111) [68, 69]. In this study, hydrogen molecules impinging on an almost complete hydrogen overlayer did not adsorb dissociatively in hydrogen dimer vacancies [68, 69]. Instead, aggregates of three or more vacancies were required for the dissociative adsorption of  $H_2$ . A subsequent DFT study demonstrated that the dissociative adsorption of  $H_2$  in a hydrogen dimer vacancy

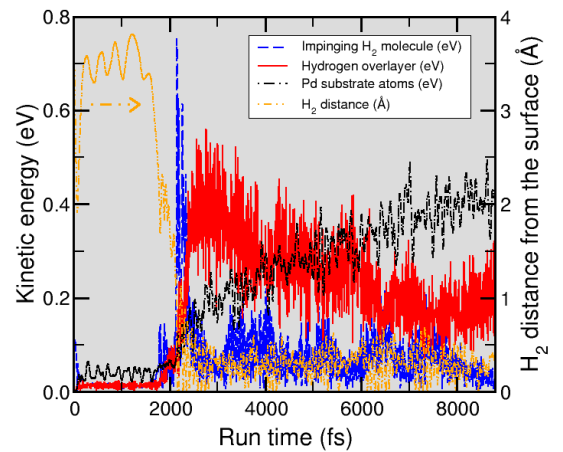


FIG. 2: Energy redistribution and  $H_2$  center of mass distance from the surface along a particular trajectory for a  $H_2$  molecule impinging with  $E_{kin} = 0.1$  eV on a hydrogen-covered Pd(100) surface with  $\theta_H = 7/9$ .

should still be exothermic [70], but because of the repulsive interaction between the hydrogen atoms the dissociation is no longer non-activated but becomes hindered by small barriers.

Note that the  $H_2$  adsorption process requires the dissipation of more than 1 eV [70]. It was speculated that the energy transfer to substrate phonons and electron hole-pair excitations could be suppressed due to surface stiffening or the modification of the electronic band structure, respectively, caused by the hydrogen overlayer [71]. However, no simulations were available that could model both the dissociative adsorption and the energy transfer to the substrate so that this speculation could neither be verified nor falsified.

These findings motivated AIMD simulations addressing the dissociative adsorption of  $H_2$  on hydrogen-precovered Pd(111) [60] and Pd(100) with dimer and trimer vacancies. They are ideally suited to model chemical reactions and energy dissipation due to surface recoil on an equal footing. In a first step, on Pd(111) a small initial kinetic energy of 0.02 eV corresponding to the thermal velocities of the STM experiments was used. And indeed, no single adsorption event in a hydrogen dimer vacancy (2V) on Pd(111) within a  $(3 \times 3)$  surface geometry was found. These AIMD results confirm the experiment [68] and provide an explanation for the experimental findings: At the low  $H_2$  gas temperatures used in the experiment the impinging  $H_2$  molecules did not have enough kinetic energy to cross the dissociation barrier. The more open trimer vacancies, on the other hand, allow a facile dissociation of  $H_2$ .

Figure 1 also includes the sticking probabilities on hydrogen-covered Pd(111) with a dimer vacancy (2V) and with trimer vacancies on centered either around a hollow site ( $3V_H$ ) or a Pd top site ( $3V_T$ ) for  $E_{kin} =$

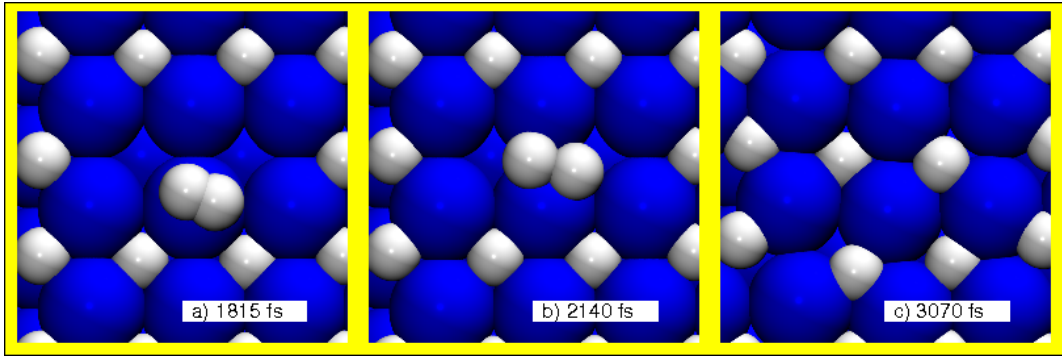


FIG. 3: Snapshots of the AIMD trajectory of  $\text{H}_2$  impinging on hydrogen-precovered Pd(100) whose energy distribution is plotted in Fig. 2. The initial hydrogen coverage is  $\theta_{\text{H}} = 7/9$  within a  $(3 \times 3)$  surface periodicity.

0.1 eV. At these higher kinetic energy,  $\text{H}_2$  adsorbs also on a dimer vacancy with a relative sticking probability of 0.05 for a surface coverage of  $\Theta_{\text{H}} = 7/9$ . This shows that the assumption that aggregates of three or more vacancies were required for the dissociative adsorption of  $\text{H}_2$  is not justified.

On the more open and thus more reactive Pd(100) surface,  $\text{H}_2$  even spontaneously dissociates in a dimer vacancy, and at  $E_{\text{kin}} = 0.1$  eV the relative sticking probability 0.23 at  $\Theta_{\text{H}} = 7/9$  is much larger than on Pd(111). The energy redistribution along a typical trajectory of  $\text{H}_2$  eventually entering a dimer vacancy on Pd(100) is plotted in Fig. 2. After impinging on the hydrogen-covered Pd(100) surface, the  $\text{H}_2$  becomes first dynamically trapped [8, 17] due to energy transfer from the translational energy to internal degrees of freedom, mainly the rotation. At about 1.8 ps, the molecule enters a weakly bound molecular precursor state above the top sites. This state that is shown in Fig. 3a stabilized due to the poisoning effects of the pre-adsorbed hydrogen atoms, very similar to the one already identified at the hydrogen-covered stepped Pd(210) surface [9, 10]. It has not been detected experimentally yet, however, one should be able to identify it at low surface temperatures by, e.g., isotope exchange experiments.

At 2.1 ps, the hydrogen molecule enters the molecular chemisorption well (Fig. 3b) thereby gaining approximately 0.8 eV. This energy is then rather quickly transferred to the hydrogen substrate atoms. Figure 3c illustrates that the adsorbed hydrogen atoms exhibit large vibrational amplitudes around their energy minimum positions. The energy transfer to the much heavier Pd substrate atoms takes much longer, only 6 ps after the  $\text{H}_2$  molecule entered the atomic chemisorption wells, the kinetic energy of the Pd atoms levels off. Interestingly enough, AIMD simulations with only fixed Pd atoms and with only fixed hydrogen overlayer atoms demonstrated that both the motion of the hydrogen atoms and the Pd atoms contribute to the high sticking probability at the precovered surfaces [60]. A detailed analysis of the adsorption dynamics indicates that it is not only energy

transfer processes alone that enhance the sticking probability of  $\text{H}_2$  molecules, but also substrate recoil and relaxation effects in the highly corrugated potential energy surface play a role.

In the previous discussion, we presented the energetics associated with the process of a hydrogen molecule entering a hydrogen dimer vacancy. In fact, on Pd(100) it turns out that even not a dimer vacancy is required to dissociate  $\text{H}_2$ , a single hydrogen vacancy is enough [72]. This is demonstrated in Fig. 4, where snapshots of an AIMD trajectory of  $\text{H}_2$  on  $c(2 \times 2)\text{H}/\text{Pd}(100)$  are shown. This surface does not have adjacent hydrogen vacancies. First the  $\text{H}_2$  becomes trapped in the molecular state above the top site for about 10 ps (see Fig. 4a). After 10 ps, one of the two hydrogen atoms of the  $\text{H}_2$  molecule enters a vacancy while the other hydrogen atom stays in a bridge position (Fig. 4b). This bridge-site hydrogen might in fact be a candidate to explain the saturation coverage of hydrogen on Pd(100) that is larger than one, as measured by Behm *et al.* [38] (see Fig. 1). Since hydrogen can only desorb recombinatively, this hydrogen will stay on the surface as long as it does not find another weakly bound H atom. However, it is rather mobile and can propagate in an exchange-like mechanism as first described for Al atoms on Al(111) [73]. This means that the bridge-site hydrogen atom replaces one of the adsorbed hydrogen atoms at an adjacent four-fold hollow sites which is pushed up (Fig. 4c). Thus the hydrogen atoms at the bridge site can travel along the surface until they find an empty four-fold hollow site where they then stay. Through this mechanism  $\text{H}_2$  molecules can adsorb dissociatively on hydrogen-covered Pd(100), even if there are only isolated vacancies present.

Currently, there has been a renewed interest in the hydrogen absorption in metals [28] in the context of the hydrogen technology. It is important to realize that there are still a lot of open issues with respect to hydrogen storage [74]. According to experiments, on Pd hydrogen first adsorbs *on* the surface before bulk absorption starts [21]. DFT calculations have confirmed this picture by demonstrating that hydrogen subsurface absorption

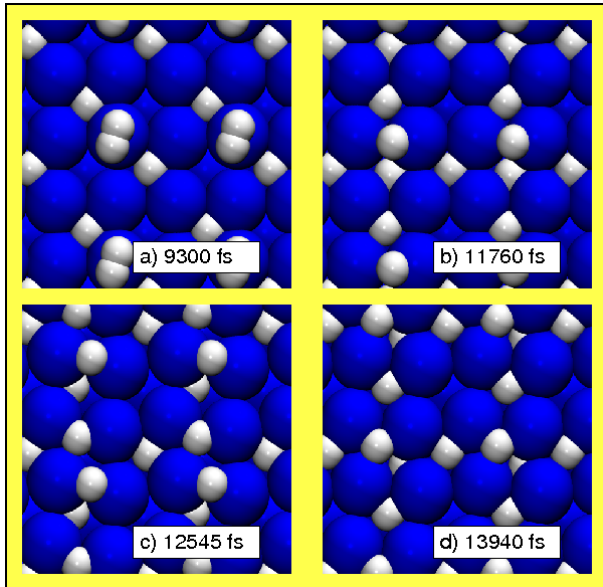


FIG. 4: Snapshots of an AIMD trajectory of  $\text{H}_2$  impinging on hydrogen-precovered  $c(2 \times 2)\text{H}/\text{Pd}(100)$  corresponding to an initial hydrogen coverage of  $\theta_{\text{H}} = 1/2$ , i.e., there are two separate hydrogen vacancies in the surface unit cell.

is energetically less favorable than adsorption on the surface [10]; furthermore, the penetration into the Pd bulk is hindered by barriers of considerable height [28].

According to the AIMD simulations, hydrogen subsurface penetration into Pd does not occur spontaneously. It is hindered by an activation barrier making it to a rare event at an initial kinetic energy of 0.1 eV. Still, several subsurface penetration events were observed in the AIMD simulations. Interestingly, most of these events involved a concerted motion of hydrogen atoms. In fact, the trajectory depicted in Fig. 4 involves such a subsurface penetration event which is illustrated in Fig. 4d. At about 14 ps, one of the hydrogen atoms starts to propagate towards a subsurface site. At the same time, the four-fold hollow site that is about to be emptied, will be refilled by an hydrogen atom from the neighboring bridge site. It looks as if the upper hydrogen atom pushes the lower hydrogen atom down. However, the driving force is rather that it is a combined bond-making/bond breaking process. An isolated subsurface penetration event requires to overcome a barrier of about 0.6 eV, since the hydrogen has to leave the energetically favorable four-fold hollow site and propagate through a low-coordinated transition state also involving strain effects. In the concerted motion, the energy cost of going through the low-coordinated transition state is compensated to a large extent by the energy gain when the bridge-site hydrogen atom enters the four-fold hollow site that is about to be emptied. The combined effect results in a concerted process that is hindered by a barrier of less than 0.1 eV. Such a concerted motion provides an explanation for the facile hydrogen subsurface penetration once the surface

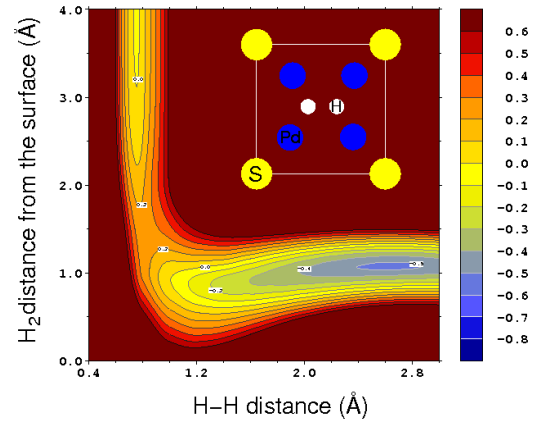


FIG. 5: Two-dimensional cut through the potential energy surface of  $\text{H}_2/\text{S}(2 \times 2)/\text{Pd}(100)$  derived from DFT calculations as a function of the H-H distance and the  $\text{H}_2$  distance from the surface. The inset illustrates the molecular orientation and lateral center of mass position. The contour spacing is 0.1 eV.

is almost covered by hydrogen.

#### IV. $\text{H}_2$ ADSORPTION DYNAMICS ON SULFUR-PRECOVERED $\text{Pd}(100)$

So far we have concentrated on the  $\text{H}_2$  dissociation dynamics on hydrogen-precovered  $\text{Pd}(100)$ . However, it is well-known that other species on the surface can also significantly influence reaction probabilities on surfaces. They can either poison or promote reactions on surfaces. Sulfur is known to lead to a poisoning of the platinum-based car-exhaust catalyst, but the poisoning effect of sulfur is not restricted to oxidation reactions on platinum surfaces. On  $\text{Pd}(100)$ , sulfur adsorption leads to a significant reduction of the hydrogen dissociation probability [6, 12].

Because of the presence of sulfur,  $\text{H}_2$  dissociation on Pd is no longer non-activated [6, 12, 40]. Figure 5 shows a two-dimensional cut through the PES of  $\text{H}_2$  interacting with  $\text{S}(2 \times 2)/\text{Pd}(100)$  derived from PAW-DFT calculations. The minimum energy barrier towards dissociative adsorption is about 0.25 eV. This is about 0.1 eV higher than the results of previous calculations [43, 75] which is caused by the different technical setups of the simulations, mainly the different treatment of the core electrons [76].

An analysis of the electronic structure of the interacting system demonstrates that the poisoning of sulfur is due to a combination of direct and indirect effects [43, 75]. Since sulfur is strongly bound to  $\text{Pd}(100)$  it first of all blocks sites at which no further reaction can take place. In the vicinity of the sulfur atoms the direct repulsion between  $\text{H}_2$  and sulfur leads to a dramatic increase in the dissociation barrier height. But secondly, it

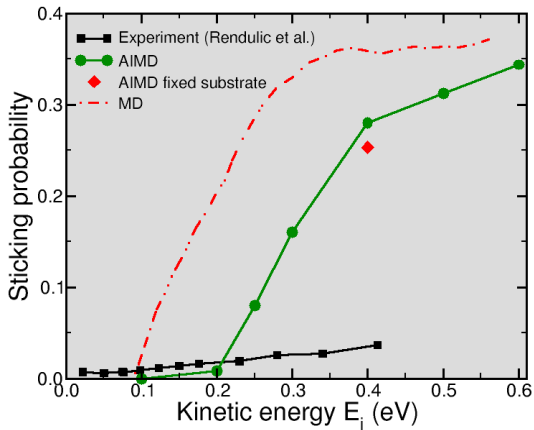


FIG. 6: The measured sticking probability of  $\text{H}_2$  on S-covered Pd(100) [6] is compared to the results of classical MD simulation [45] based on a parameterization of DFT results [43, 75] and to the results of AIMD simulations. For  $E_{\text{kin}} = 0.4 \text{ eV}$ , additional AIMD runs with the substrate kept fixed were performed.

also modifies the electronic structure of the Pd substrate. The interaction of sulfur with Pd leads to a down-shift of the Pd  $d$ -states. As a consequence [77], even further away from the sulfur atoms as for example at the four-fold hollow site depicted in Fig. 5 dissociation barriers are built up.

In order to study the dynamical consequences of the sulfur-poisoning on the hydrogen adsorption dynamics, six-dimensional quantum and classical dynamical study were performed [40, 44, 45] on a parameterization of previous DFT calculations [43, 75]. Figure 6 shows the calculated classical sticking probabilities as a function of the initial kinetic energies for initially non-rotating and non-vibrating molecules which are denoted by MD in the legends. In addition, the results of recent AIMD simulations are included. Compared to the MD simulations, the AIMD results are shifted towards higher energies by 0.1 eV which is exactly the difference in the minimum barrier heights using the two different DFT setups on which the energetics of the dynamical simulations are based.

More importantly, the similar qualitative behavior of the results of the MD and the AIMD simulations demonstrates that the parameterization of the  $\text{H}_2/\text{S}(2 \times 2)/\text{Pd}(100)$  interaction which has only been adjusted at the high-symmetry sites captures the essential features in this activated system. In a non-activated system such as  $\text{H}_2$  dissociation on clean Pd(100), such a parameterization restricted to high-symmetry points is not sufficient since in such a system without a minimum barrier the dynamics sensitively depend on extended regions of the PES [55, 56, 60] and not only on the region close to the minimum barrier.

In Fig. 6, for  $E_{\text{kin}} = 0.4 \text{ eV}$  the sticking probability according to AIMD simulations with the surface degrees

kept frozen are included. There is only a small difference to the result with the uppermost surface atoms allowed to move. This is again in contrast to the results for the non-activated  $\text{H}_2/\text{Pd}(100)$  system where in the dynamical trapping energy transfer and recoil processes play an important role whereas for the activated  $\text{H}_2/\text{S}(2 \times 2)/\text{Pd}(100)$  system they obviously do not matter.

In addition to the sticking probability for normal incidence, the experimentally observed dependence of the  $\text{H}_2$  interaction dynamics with respect to the rotational and vibrational degrees of freedom and with respect to the orientation of the molecules was reproduced by the quantum and classical simulations on the parameterized PES [40, 44, 45]. Still it should be noted that there are large significant quantitative and qualitative differences, as far as the sticking probability is concerned. The measured probabilities are much smaller than the calculated ones. It is true that the dynamical simulations are only of approximate nature. The calculated PES might not be fully correct due to problems associated with current DFT functionals [78]. Furthermore, the neglect of electronic excitations could have an influence on the accuracy of the results. However, it should also be noted that experimentally the preparation of an ordered  $(2 \times 2)$  sulfur overlayer on Pd(100) is not trivial [6, 40]. It is often prepared by just heating up the Pd sample leading to a segregation of the sulfur dissolved in the bulk Pd crystal to the surface [6].

Sulfur tends to form a  $c(2 \times 2)$  overstructure on Pd(100) [40] corresponding to a higher sulfur coverage of  $\Theta_{\text{S}} = 0.5$ . At such a high sulfur coverage, Pd is totally unreactive with respect to hydrogen dissociation. This would explain the low sticking probability observed in the experiment [6]. It is certainly desirable that additional molecular beam experiments of hydrogen dissociation on sulfur-covered Pd with a well-defined sulfur coverage are performed.

## V. RELAXATION DYNAMICS OF DISSOCIATED $\text{H}_2$ MOLECULES

In the previous sections I have discussed the dissociation of  $\text{H}_2$  on pre-covered Pd surfaces. The main focus was on the question whether  $\text{H}_2$  dissociates on Pd or not, but the fate of the hydrogen atoms after the dissociation was not really considered. However, directly after the dissociation when the atoms enter the atomic adsorption wells, they gain a significant amount of energy. For  $\text{H}_2/\text{Pd}$ , this amounts to about 1 eV for the two H atoms together and thus gives rise to the formation of “hot” atoms, i.e., atoms with energies much larger than thermal energies. Now if the hydrogen atoms enter atomic adsorption wells surrounded by occupied adsorption sites, they hardly can propagate any further.

On a clean surface, however, these hot atoms can use their kinetic energy in order to travel along the surface

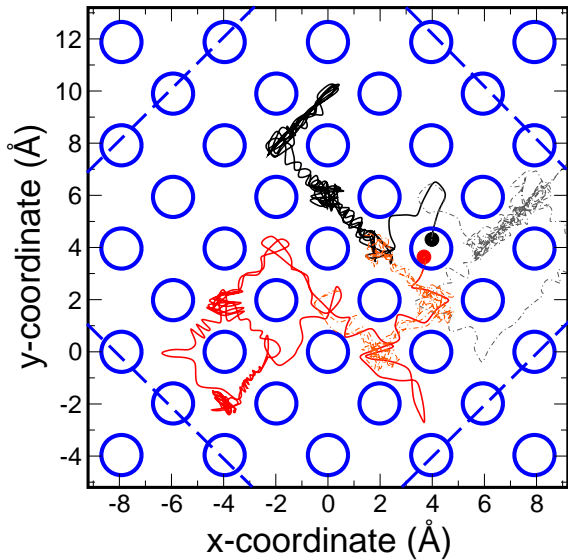


FIG. 7: Trajectories of the dissociative adsorption event of  $H_2$  impinging on clean Pd(100) determined by AIMD simulations within a  $(6 \times 6)$  surface unit cell [79]. The initial kinetic energy was 0.2 eV. The total run time was 2.5 ps. Two sets of trajectories with the same initial conditions are shown. The full lines correspond to the joint motion of the two hydrogen atoms while for the dash-dotted lighter lines the trajectories were computed individually after the two hydrogen atoms reached a separation of 2.5 Å. The surface unit cell of the simulations is indicated by the dashed blue line.

since the barrier for diffusion is much lower than their excess energy directly after entering the adsorption well. The mean free path of these hot atoms is for example relevant for catalytic reactions on surfaces since it determines whether adjacent species can react directly after the dissociative adsorption of one of the species or whether some diffusive motion is required before any further reaction can occur.

In order to address the distance of the hydrogen atoms after dissociative adsorption on clean Pd(100), AIMD simulations of  $H_2$  impinging on Pd(100) using a rather large  $(6 \times 6)$  surface unit cell were performed [79]. An initial kinetic energy of 0.2 eV was chosen to avoid any trapping into a dynamical precursor as depicted in Fig. 4a. The full lines in Fig. 7 show one typical trajectory of the dissociative adsorption of  $H_2$ . So far, simulations addressing the relaxation of hot atoms after dissociation have only modeled the motion of single atoms with initial velocities considered to be typical for dissociation fragments directly after the bond-breaking process [11, 80]. In fact, the dash-dotted lines in Fig. 7 correspond to such a simulation in which the motion of the two hydrogen atoms was determined individually after their separation exceeded 2.5 Å.

As Fig. 7 illustrates, these two different kind of trajectories differ quite significantly. This means that any single trajectories depends sensitively on the particular conditions of the runs. In particular the mutual interac-

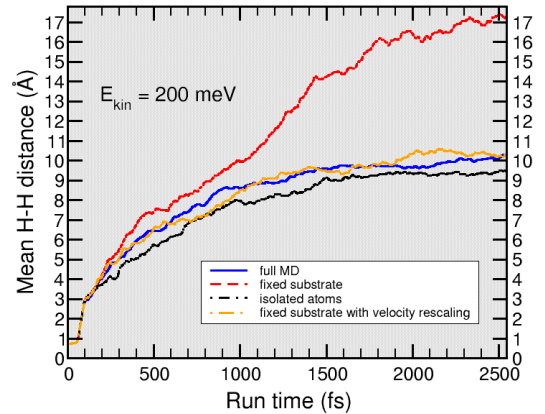


FIG. 8: Mean lateral distance of the two hydrogen atoms upon the  $H_2$  dissociative adsorption on Pd(100) as a function of the run time determined by averaging over AIMD trajectories for different computational setups (see text). In each case, at least 75 trajectories were determined [79].

tion between the two fragments can be quite important for a specific dissociative adsorption event. However, on the average this mutual interaction does not seem to matter for the final distance of the two hydrogen atoms after dissociative adsorption. This is demonstrated in Fig. 8 where the mean distance of the hydrogen atoms after dissociative adsorption as a function of time averaged over at least 75 trajectories is shown. To reduce the computational cost, only three Pd layers were considered in the simulations but simulations with five Pd layers yield almost identical results [79].

The mean results for the combined and the isolated motion of the two hydrogen atoms hardly differ: after about 1.5 ps it reaches a value of about 10 Å and does not increase any further. This corresponds to about three to four Pd lattice units. Also surface relaxation effects play no important role as reflected by the results of simulations with a fixed substrate but velocity rescaling in order to take account of the energy dissipation which are included in Fig. 8. Only if no energy dissipation is considered in the simulations with a fixed substrate, the mean distance differs quite substantially. This shows that it is basically the energy transfer to the substrate that determines the mean distance of the two fragments after dissociative adsorption. For heavier species such as oxygen atoms [81, 82] that dissipate their energy more quickly to substrate phonons, the separations determined in this study should provide an upper bound for the distance they travel after dissociative adsorption provided the corresponding potential energy surface is similar.

## VI. CONCLUSIONS

In this brief review, recent *ab initio* molecular dynamics studies of the dissociative adsorption of  $H_2$  on clean

and precovered Pd(100) were presented. The calculations showed that the sticking probability depends sensitively on the particular configuration of the pre-adsorbed atoms. These unbiased simulations helped to identify novel processes and structures such as bridge-site hydrogen on hydrogen-covered Pd(100) that can travel in an exchange-like fashion or the concerted mechanism of hydrogen subsurface penetration. Furthermore it was demonstrated that the mean distance of the hydrogen atoms on clean Pd(100) only depends on the energy dissipation. These results illustrate that AIMD simulations are well-suited in order to unravel details of reaction dynamics at complex surface structures that are not acces-

sible to experiment.

### Acknowledgments

Some of the calculations presented in this brief review were made possible through a grant of computer time at the John von Neumann Institute for Computing in Jülich. Additional computational resources have been provided by the bwGRiD project of the Federal State of Baden-Württemberg/Germany.

- 
- [1] A. Groß, Surf. Sci. Rep. **32**, 291 (1998).  
 [2] G.-J. Kroes, A. Groß, E. J. Baerends, M. Scheffler, and D. A. McCormack, Acc. Chem. Res. **35**, 193 (2002).  
 [3] K. Christmann, Surf. Sci. Rep. **9**, 1 (1988).  
 [4] A. Eichler, J. Hafner, A. Groß, and M. Scheffler, Chem. Phys. Lett. **311**, 1 (1999).  
 [5] R. J. Behm, K. Christmann, and G. Ertl, Surf. Sci. **99**, 320 (1980).  
 [6] K. D. Rendulic, G. Anger, and A. Winkler, Surf. Sci. **208**, 404 (1989).  
 [7] A. Groß and M. Scheffler, Chem. Phys. Lett. **263**, 567 (1996).  
 [8] A. Groß and M. Scheffler, J. Vac. Sci. Technol. A **15**, 1624 (1997).  
 [9] P. K. Schmidt, K. Christmann, G. Kresse, J. Hafner, M. Lischka, and A. Groß, Phys. Rev. Lett. **87**, 096103 (2001).  
 [10] M. Lischka and A. Groß, Phys. Rev. B **65**, 075420 (2002).  
 [11] N. Pineau, H. F. Busnengo, J. C. Rayez, and A. Salin, J. Chem. Phys. **122**, 214705 (2005).  
 [12] M. L. Burke and R. J. Madix, Surf. Sci. **237**, 1 (1990).  
 [13] M. Beutl, M. Riedler, and K. D. Rendulic, Chem. Phys. Lett. **247**, 249 (1995).  
 [14] E. Kampshoff, N. Waelchli, A. Menck, and K. Kern, Surf. Sci. **360**, 55 (1996).  
 [15] R. A. Olsen, G. J. Kroes, O. M. Løvvik, and E. J. Baerends, J. Chem. Phys. **107**, 10652 (1997).  
 [16] M. Gostein and G. O. Sitz, J. Chem. Phys. **106**, 7378 (1997).  
 [17] H. F. Busnengo, W. Dong, and A. Salin, Chem. Phys. Lett. **320**, 328 (2000).  
 [18] H. F. Busnengo, W. Dong, P. Sautet, and A. Salin, Phys. Rev. Lett. **87**, 127601 (2001).  
 [19] D. Wetzig, M. Rutkowski, H. Zacharias, and A. Groß, Phys. Rev. B **63**, 205412 (2001).  
 [20] A. Lozano, A. Groß, and H. F. Busnengo, Phys. Chem. Chem. Phys. **11**, 5814 (2009).  
 [21] U. Muschiol, P. K. Schmidt, and K. Christmann, Surf. Sci. **395**, 182 (1998).  
 [22] D. Tománek, S. Wilke, and M. Scheffler, Phys. Rev. Lett. **79**, 1329 (1997).  
 [23] J. Yoshinobu, H. Tanaka, and M. Kawai, Phys. Rev. B **51**, 4529 (1995).  
 [24] S. H. Kim, H. L. Meyerheim, J. Barthel, J. Kirschner, J. Seo, and J.-S. Kim, Phys. Rev. B **71**, 205418 (2005).  
 [25] A. Groß, Appl. Phys. A **67**, 627 (1998).  
 [26] R. J. Behm, V. Penka, M.-G. Cattania, K. Christmann, and G. Ertl, J. Chem. Phys. **78**, 7486 (1983).  
 [27] M.-G. Cattania, V. Penka, R. J. Behm, K. Christmann, and G. Ertl, Surf. Sci. **126**, 382 (1983).  
 [28] A. Pundt and R. Kirchheim, Annu. Rev. Mater. Res. **36**, 555 (2006).  
 [29] F. Favier, E. C. Walter, M. P. Zach, T. Benter, and R. M. Penner, Science **293**, 2227 (2001).  
 [30] V. Ledentu, W. Dong, P. Sautet, A. Eichler, and J. Hafner, Phys. Rev. B **57**, 12482 (1998).  
 [31] R. A. Olsen, P. H. T. Philipsen, E. J. Baerends, G. J. Kroes, and O. M. Løvvik, J. Chem. Phys. **106**, 9286 (1997).  
 [32] W. Dong, V. Ledentu, P. Sautet, A. Eichler, and J. Hafner, Surf. Sci. **411**, 123 (1998).  
 [33] S. Wilke, D. Hennig, R. Löber, M. Methfessel, and M. Scheffler, Surf. Sci. **307**, 76 (1994).  
 [34] J.-F. Paul and P. Sautet, Phys. Rev. B **53**, 8015 (1996).  
 [35] R. Löber and D. Hennig, Phys. Rev. B **55**, 4761 (1997).  
 [36] R. Behm, K. Christmann, G. Ertl, M. V. Hove, P. Thiel, and W. Weinberg, Surf. Sci. **88**, L59 (1979).  
 [37] J. Quinn, Y. S. Li, D. Tian, H. Li, F. Jona, and P. M. Marcus, Phys. Rev. B **42**, 11348 (1990).  
 [38] R. J. Behm, K. Christmann, G. Ertl, and M. A. Van Hove, J. Chem. Phys. **73**, 2984 (1980).  
 [39] M. Rutkowski, D. Wetzig, and H. Zacharias, Phys. Rev. Lett. **87**, 246101 (2001).  
 [40] M. Rutkowski, D. Wetzig, H. Zacharias, and A. Groß, Phys. Rev. B **66**, 115405 (2002).  
 [41] S. Wilke and M. Scheffler, Surf. Sci. **329**, L605 (1995).  
 [42] S. Wilke, M. H. Cohen, and M. Scheffler, Phys. Rev. Lett. **77**, 1560 (1996).  
 [43] C. M. Wei, A. Groß, and M. Scheffler, Phys. Rev. B **57**, 15572 (1998).  
 [44] A. Groß, C. M. Wei, and M. Scheffler, Surf. Sci. **416**, L1095 (1998).  
 [45] A. Groß and M. Scheffler, Phys. Rev. B **61**, 8425 (2000).  
 [46] M. Lischka, C. Mosch, and A. Groß, Surf. Sci. **570**, 227 (2004).  
 [47] A. Groß, S. Wilke, and M. Scheffler, Phys. Rev. Lett. **75**, 2718 (1995).  
 [48] G.-J. Kroes, E. J. Baerends, and R. C. Mowrey, Phys. Rev. Lett. **78**, 3583 (1997).  
 [49] G.-J. Kroes, Prog. Surf. Sci. **60**, 1 (1999).



- [50] H. F. Busnengo, E. Pijper, M. F. Somers, G. J. Kroes, A. Salin, R. A. Olsen, D. Lemoine, and W. Dong, *Chem. Phys. Lett.* **356**, 515 (2002).
- [51] A. Groß and M. Scheffler, *Phys. Rev. B* **57**, 2493 (1998).
- [52] G. Wiesenekker, G.-J. Kroes, and E. J. Baerends, *J. Chem. Phys.* **104**, 7344 (1996).
- [53] H. F. Busnengo, A. Salin, and W. Dong, *J. Chem. Phys.* **112**, 7641 (2000).
- [54] A. Groß and M. Scheffler, *Phys. Rev. B* **57**, 2493 (1998).
- [55] S. Lorenz, A. Groß, and M. Scheffler, *Chem. Phys. Lett.* **395**, 210 (2004).
- [56] S. Lorenz, M. Scheffler, and A. Groß, *Phys. Rev. B* **73**, 115431 (2006).
- [57] A. Groß, M. Scheffler, M. J. Mehl, and D. A. Papaconstantopoulos, *Phys. Rev. Lett.* **82**, 1209 (1999).
- [58] A. Groß, M. Bockstedte, and M. Scheffler, *Phys. Rev. Lett.* **79**, 701 (1997).
- [59] L. C. Ciacchi and M. C. Payne, *Phys. Rev. Lett.* **92**, 176104 (2004).
- [60] A. Groß and A. Dianat, *Phys. Rev. Lett.* **98**, 206107 (2007).
- [61] G. Kresse and J. Furthmüller, *Phys. Rev. B* **54**, 11169 (1996).
- [62] J. P. Perdew, J. A. Chevary, S. H. Vosko, K. A. Jackson, M. R. Pederson, D. J. Singh, and C. Fiolhais, *Phys. Rev. B* **46**, 6671 (1992).
- [63] J. P. Perdew, K. Burke, and M. Ernzerhof, *Phys. Rev. Lett.* **77**, 3865 (1996).
- [64] D. Vanderbilt, *Phys. Rev. B* **41**, 7892 (1990).
- [65] P. E. Blöchl, *Phys. Rev. B* **50**, 17953 (1994).
- [66] A. Groß, *Theoretical surface science – A microscopic perspective* (Springer, Berlin, 2009), 2nd ed.
- [67] H. J. Kreuzer, *J. Chem. Phys.* **104**, 9593 (1996).
- [68] T. Mitsui, M. K. Rose, E. Fomin, D. F. Ogletree, and M. Salmeron, *Nature* **422**, 705 (2003).
- [69] T. Mitsui, M. K. Rose, E. Fomin, D. F. Ogletree, and M. Salmeron, *Surf. Sci.* **540**, 5 (2003).
- [70] N. Lopez, Z. Lodziana, F. Illas, and M. Salmeron, *Phys. Rev. Lett.* **93**, 146103 (2004).
- [71] S. Holloway, *Surf. Sci.* **540**, 1 (2003).
- [72] A. Lozano, A. Groß, and H. F. Busnengo, *Phys. Rev. Lett.*, submitted for publication.
- [73] P. J. Feibelman, *Phys. Rev. Lett.* **65**, 729 (1990).
- [74] L. Schlapbach and A. Züttel, *Nature* **415**, 353 (2001).
- [75] S. Wilke and M. Scheffler, *Phys. Rev. Lett.* **76**, 3380 (1996).
- [76] S. Sakong and A. Groß, *J. Phys. Chem. A* **111**, 8814 (2007).
- [77] B. Hammer and J. K. Nørskov, *Surf. Sci.* **343**, 211 (1995).
- [78] A. J. Cohen, P. Mori-Sánchez, and W. Yang, *Science* **321**, 792 (2008).
- [79] A. Groß, *Phys. Rev. Lett.*, submitted for publication.
- [80] C. Engdahl and G. Wahnström, *Surf. Sci.* **312**, 429 (1994).
- [81] H. Brune, J. Wintterlin, R. J. Behm, and G. Ertl, *Phys. Rev. Lett.* **68**, 624 (1992).
- [82] J. Wintterlin, R. Schuster, and G. Ertl, *Phys. Rev. Lett.* **77**, 123 (1996).